Carbohydrate Polymers 96 (2013) 417–425

Contents lists available at SciVerse ScienceDirect

Carbohydrate Polymers

journal homepage: www.elsevier.com/locate/carbpol

Bioconversion to chitosan: A two stage process employing chitin deacetylase from *Penicillium oxalicum* SAE_M-51

Nidhi Pareek[1], V. Vivekanand[2], Pragati Agarwal, Samta Saroj, Rajesh P. Singh*

Department of Biotechnology, Indian Institute of Technology Roorkee, Roorkee 247667, Uttarakhand, India

ARTICLE INFO

Article history:
Received 10 January 2013
Received in revised form 25 March 2013
Accepted 6 April 2013
Available online 16 April 2013

Keywords:
Chitin
Chitosan
Penicillium oxalicum
Chitin deacetylase
Central composite design

ABSTRACT

Chitin deacetylase from *Penicillium oxalicum* SAE_M-51 was evaluated for bioconversion of chitin to chitosan in a two stage chemical and enzymatic process. Variations in morphology, crystallinity and thermal properties following chemical treatment were evaluated by scanning electron microscopy, X-ray diffraction, differential scanning calorimetry and thermogravimetric analysis. Degree of deacetylation of the substrates was determined using FT-IR and elemental analysis. The pretreatment of substrate led to the decrease in crystallinity and formation of amorphous chitinous substrates to facilitate enzyme reaction. The treated chitin was further subjected to enzymatic deacetylation employing chitin deacetylase from *P. oxalicum* SAE_M-51 to produce chitosan with considerably higher degree of deacetylation. Maximum deacetylation (79.52%) was achieved using superfine chitin, owing to its porous structure and low crystallinity. Further, derivation of reaction variables, i.e. substrate amount and enzyme dose through full-factorial central composite design led to enhanced degree of deacetylation with formation of 90% deacetylated chitosan.

1. Introduction

Chitosan, the linear and partly acetylated (1-4)-2-amino-2-deoxy-β-D-glucan, is isolated from marine chitin (Muzzarelli, 2011; Muzzarelli et al., 2012). It is a polymer of choice for various modern bio-based industrial applications such as drug delivery, nutraceutical, cosmetics, waste water treatment, and agriculture (Aranaz et al., 2009). Functional properties and in turn industrial utility of chitosan depends on the degree and distribution of deacetylated subunits (Kumar, Muzzarelli, Muzzarelli, Sashiwa, & Domb, 2004; Zhao, Park, & Muzzarelli, 2010). Most of the commercially available chitosan is obtained from thermo-alkaline deacetylation of chitin from crustacean shells (Focher, Beltrame, Naggi, & Torri, 1990; Nessa et al., 2010; No, Cho, Kim, & Meyers, 2000). The process utilizes large volume of concentrated alkali solution at high temperature in both homogeneous and heterogeneous conditions. A product with high degree of deacetylation (DDA) can be produced from the chemical treatment but the process compromises with the product quality and generates heterogeneous range of products due to depolymerization of chitin backbone. In addition, it also shares disadvantages of most of the chemical processes like tedious to control and environmentally unsafe. Enzymatic deacetylation is a competent, controlled, non-degradative and well-defined solution to the chemical process. Chitin deacetylase (CDA, EC 3.5.1.41) catalyzes the deacetylation of monomeric acetyl glucosamine units of chitin by multiple attack mechanism and produces high quality chitosan (Arakane, Taira, Ohnuma, & Fukamizo, 2012; Gou, Dong, Zeng, & Zhang, 2012; Liu & He, 2011; Tsigos, Martinou, Kafetzopoulos, & Bouriotis, 2000; Zhao et al., 2010).

Till date, CDA production and enzymatic deacetylation has been studied by several groups (Aye, Karuppuswamy, Ahamed, & Stevens, 2006; Beaney, Gan, Magee, Flealy, & Lizardi-Mendoza, 2007; Caufrier, Martinou, Dupont, & Bouriotis, 2003; Martinou, Kafetzopoulos, & Bouriotis, 1995; Tokuyasu, Ohnishi-Kameyama, & Hayashi, 1996; Win & Stevens, 2001). The enzyme has largely been found to be ineffective in deacetylating insoluble chitin substrates (Win, Pengju, & Stevens, 2000). Crystallinity and insolubility of chitin are the two major barriers that hinder the development of a productive enzymatic deacetylation process (Beaney et al., 2007; Kolodziejska, Wojtasz-Pajak, Ogonowska, & Sikorski, 2000). Both the parameters affect substrate accessibility to the enzyme and impede the enzyme action on interior acetyl group, therefore negatively affect the production of highly deacetylated chitosan species. Pretreatment of chitinous materials prior to enzyme addition may lead to conformational modification of the parent polymer, which in turn enhance the enzyme substrate interaction and hence the subsequent deacetylation. Chitin can be treated by both physical

* Corresponding author. Tel.: +91 1332 285792; fax: +91 1332 273560.
E-mail address: rpsbsfbs@iitr.ernet.in (R.P. Singh).
[1] Present address: Department of Chemistry, Umeå University, SE-90183 Umeå, Sweden.
[2] Present address: Protein Engineering and Proteomics Group, Department of Chemistry, Biotechnology and Food Sciences, Norwegian University of Life Sciences, Ås 1430, Norway.

0144-8617/$ – see front matter © 2013 Elsevier Ltd. All rights reserved.
http://dx.doi.org/10.1016/j.carbpol.2013.04.005

Table 1a
Ranges of concentrations of variables analyzed using CCD.

Variable	Component	Levels ($g l^{-1}$)				
		$-\alpha$	−1	0	+1	$+\alpha$
X_1	Amount of substrate (g)	1.00	2.00	3.00	4.00	5.00
X_2	Enzyme dose (U)	20	40	60	80	100

$\alpha = 2^{k/4}$, $k = 2$, $\alpha = 1.414$.

and chemical means, where physical treatments such as heating, grinding and sonication have not been reasonably effective (Beaney et al., 2007; Win & Stevens, 2001). On the other hand, chemical treatments had resulted into significant loss of crystallinity; hence, more amorphous substrates were generated for enzymatic bioconversion (Beaney et al., 2007). Furthermore, recent studies on the chitin binding proteins (CBPs) provided new insights to enhance the substrate accessibility and achieve higher degree of deacetylation. The function of the proteins was first demonstrated for *Serratia marcescens* CBP21, a non-catalytic carbohydrate binding protein that catalyzes cleavage of glycosidic bonds in crystalline chitin, thus increasing substrate accessibility (Vaaje-Kolstad, Horn, van Aalten, Synstad, & Eijsink, 2005; Vaaje-Kolstad, Houston, Riemens, Eijsink, & Aalten, 2005; Vaaje-Kolstad et al., 2010). The enzymes can further be explored in concurrence with deacetylases to enhance the chitin deacetylation.

The present study enumerates the deacetylation efficacy of CDA from *Penicillium oxalicum* SAE_M-51 in a two-stage chemical and enzymatic process. The critical factors affecting the deacetylation process were further optimized using response surface methodology to produce chitosan with considerably high degree of deacetylation.

2. Materials and methods

2.1. Microorganism and enzyme production

P. oxalicum SAE_M-51 developed in our laboratory after successive stages of mutagenesis using microwave irradiation and ethidium bromide (EtBr) (Pareek, Vivekanand, Dwivedi, & Singh, 2011), was used for the production of CDA under solid-state fermentation conditions using mustard oil cake as a solid support. The enzyme was further purified from the crude culture supernatants using ion exchange chromatography prior to use for deacetylation (Pareek, Vivekanand, Saroj, Sharma, & Singh, 2012).

2.2. Deacetylation of chitin

Crystallinity of chitin is an important barrier to its enzymatic deacetylation. A two-stage chemical and enzymatic process was followed to achieve higher degree of deacetylation. The commercial crab shell chitin, procured from Sigma–Aldrich Co., USA, was subjected to various chemical treatments, following Beaney et al. (2007) with some modifications in order to decrease the crystallinity as well as to improve substrate accessibility to the enzyme.

2.2.1. Phosphoric acid treated chitin

Commercial chitin was treated with phosphoric acid (45%) at room temperature for 40 min and filtered through cheese cloth. Chitin was then precipitated by adding 6 M NaOH to pH 8.0. Afterwards, the resultant precipitate was washed several times with distilled water to attain neutral pH and freeze-dried.

2.2.2. Amorphous chitin

Chitin was treated with a cold solution consisting of NaOH (20%) and sodium dodecyl sulfate (SDS, 0.2%). It was then allowed to swell for an hour at 4 °C. Chitin slurry was kept overnight at −20 °C and neutralized with 6 N HCl. Precipitate was then collected by filtration, successively washed with ethanol, water, ethanol and acetone and freeze-dried.

2.2.3. Colloidal chitin

Crab shell chitin was allowed to react with HCl (20%) with constant agitation for 20 min at room temperature. Solution was filtered with glass wool in prechilled distilled water with constant mixing and allowed to settle. A dense white precipitate was formed, which was centrifuged at 10,000 rpm for 10 min at 4 °C. Precipitate was washed several times with cold distilled water until the pH reached to neutrality. Supernatant was discarded and colloidal chitin was freeze dried.

2.2.4. Superfine chitin

Chitin was dissolved in methanol (100 ml) with calcium chloride dihydrate (60%, w/v) overnight. Dissolved chitin was precipitated using calcium citrate solution (1%). The precipitate was then dialyzed for about 12 h and the resultant chitin was dried at 50 °C in a vacuum oven. Superfine chitin thus obtained was further treated with formic acid (25%) at room temperature and dried.

2.2.5. Enzymatic deacetylation

The deacetylation efficacy of *P. oxalicum* SAE_M-51 CDA for the aforementioned chitin substrates was evaluated by treating the chitin samples with purified enzyme preparation (24 h, 50 °C). The reaction was then analyzed in terms of amount of acetate released and the degree of deacetylation of the product. The higher is the amount of acetate released; more effective would be the enzymatic deacetylation. Among the analyzed substrates, the one that was observed to have maximum level of deacetylation was selected for further studies to derive the optimum levels of enzyme dose and substrate amount using response surface methodology (Tables 1a and 1b) to achieve maximum deacetylation.

2.3. Characterization of chitinous substrates

Following chemical treatment, modifications in chitin morphology, crystallinity, thermal stability and DDA were analyzed.

2.3.1. Scanning electron microscopy

Morphological variations in chitin following chemical pretreatment were analyzed using scanning electron microscopy. Briefly, samples were prepared by immersion in 5% (v/v) glutaraldehyde for 24 h at 4 °C and post-treated with OsO_4 1% (w/v) for 2 h at 4 °C followed by dehydration in a graded alcohol series and covered with carbon and gold prior to examination in the scanning electron microscope (SEM, LEO 435 VP, England).

2.3.2. X-ray diffraction

The X-ray diffraction measurement was utilized to determine the crystallinity of treated and untreated chitin samples and their patterns were recorded using an X-ray diffractometer (Bruker AXS D8) with Cu radiation (40 kV, 30 mA). The 2θ angle was scanned between 5° and 40° with scanning speed of 0.20 s^{-1}. The crystalline

Table 1b
Experimental design matrix for optimization of conditions for enzymatic deacetylation using CCD.

Run	X_1	X_2	Acetate released (mM)		DDA (%)	
			Observed	Predicted	Observed	Predicted
1	−1	−1	14.20	13.88	80.12	79.99
2	+1	−1	19.65	18.47	92.83	91.00
3	−1	+1	17.88	18.52	87.78	88.29
4	+1	+1	13.65	13.42	84.56	83.37
5	$-\alpha$	0	11.44	11.10	76.50	75.96
6	$+\alpha$	0	9.86	10.74	78.40	80.26
7	0	$-\alpha$	20.43	21.37	91.87	92.98
8	0	$+\alpha$	21.48	21.08	93.24	93.45
9	0	0	18.20	18.26	89.40	89.31
10	0	0	18.04	18.26	89.04	89.31
11	0	0	17.96	18.26	89.60	89.31
12	0	0	18.43	18.26	89.13	89.31
13	0	0	18.67	18.26	89.37	89.31

index (%) of the samples was determined by using following equations (Focher et al., 1990).

$$\mathrm{CrI}_{020} = \left[\frac{I_{020} - I_{am}}{I_{020}}\right] \times 100$$

$$\mathrm{CrI}_{110} = \left[\frac{I_{110} - I_{am}}{I_{110}}\right] \times 100$$

where I_{020} is the maximum intensity at $2\theta \approx 9^\circ$, I_{am} is the intensity of amorphous diffraction at $2\theta \approx 16^\circ$ and I_{110} is the maximum intensity at $2\theta \approx 20^\circ$.

2.3.3. Thermal analysis

The thermal properties of treated and untreated chitin samples were measured by TGA and DSC (Perkin Elmer, Pyris Diamond, USA). For the TGA and DSC analyses, the samples (10.0 mg) were placed in an aluminum cup and hermetically sealed. Afterwards, samples were heated from 25 to 600 °C at a heating rate of 20 °C min^{-1} under nitrogen atmosphere (10 ml min^{-1}) (Mao et al., 2004). Enthalpy (ΔH), onset (T_o), peak (T_p) and completion (T_c) temperatures were computed automatically.

2.3.4. Degree of deacetylation

2.3.4.1. Fourier-transform infrared (FT-IR) spectroscopy. The degree of deacetylation of chitin samples was determined using FT-IR. An aliquot of the sample was mixed with potassium bromide, compressed into pellets and used to record an infrared spectrum using FT-IR spectrophotometer (Perkin-Elmer 1600). The absorbance at 1655 cm^{-1} (amide-I) and at 3450 cm^{-1} (OH group) were used to calculate the DDA according to the following equation (Khan, Peh, & Cing, 2000).

$$\mathrm{DDA}\ (\%) = \left[1 - \frac{A_{1655}/A_{3450}}{1.33}\right] \times 100.$$

Factor 1.33 represents the ratio of A_{1655}/A_{3450} for fully N-acetylated chitosan.

2.3.4.2. Elemental analysis. The degree of deacetylation of the treated and untreated chitin samples was further verified by elemental analysis using EDAX (Quanta 200F, FEI, Netherlands) according to the following equation (Kassai, Arul, & Charlet, 2000)

$$\mathrm{DDA}\ (\%) = \left(1 - \left(\frac{\mathrm{C}}{\mathrm{N}}\right) - \frac{5.145}{6.816} - 5.145\right) \times 100$$

where C/N is the percent ration of carbon and nitrogen.

2.4. Acetate assay

Acetate released after enzymatic reaction was determined using commercial kit for acetic acid detection (Boehringer Mannheim/R-Biopharm Inc.; Cat. No. 10148261035). The method is based on the spectrophotometric determination of NADH formed by an enzyme-linked assay at 340 nm.

3. Results and discussion

3.1. Physical characterization of chemically treated chitin substrates

3.1.1. Morphology

Chitin before and following chemical treatment was observed to have distinct changes in the surface architecture. Commercial chitin from crab shell has a compact structure with some distinctly arranged crystalline microfibrils visible at its surface (Fig. 1a). Marginal porosity of the material makes it a poor substrate for enzymatic deacetylation. Both superfine (SF-CT) (Fig. 1b) and amorphous chitin (Am-CT) (Fig. 1c) deems to be the most amenable substrates for bio-catalytic deacetylation. The substrates lose their characteristic crystalline microfibrillar arrangement and have a porous structure which would allow the enzyme to act on acetyl groups. Phosphoric acid treated chitin (PA-CT) (Fig. 1d) and colloidal chitin (Co-CT) (Fig. 1e) had almost similar stature. The characteristic microfibrillar structure is visible in both the substrates but the level of complexity is somewhat low as some major and minor grooves are observed between fibrils in the micrographs due to the deformation of the crystalline structure of chitin. Chemical treatment had led into the loosening and swelling of chitin microfibrils, which facilitates the penetration of enzyme in subsequent deacetylation processes. Similar type of morphological modifications has also been observed by other groups (Beaney et al., 2007; Win & Stevens, 2001). Maximum defibrillation was observed in SF-CT; hence it appeared to be the most suitable substrate for enzymatic action.

3.1.2. Crystallinity

Crystallinity of chitin is a significant criterion that enables the understanding of its susceptibility toward enzymatic deacetylation. Chitin in its native state has a characteristic higher degree of crystallinity, which lowers its susceptibility toward enzymatic deacetylation. Chemical pretreatment had resulted into significant loss of crystalline structure with generation of new amorphous chitin variants. Crystallinity of chitin before and following pretreatment was determined using wide angle X-ray diffraction analysis in terms of crystalline index (CrI_{020}, CrI_{110}), by taking into account

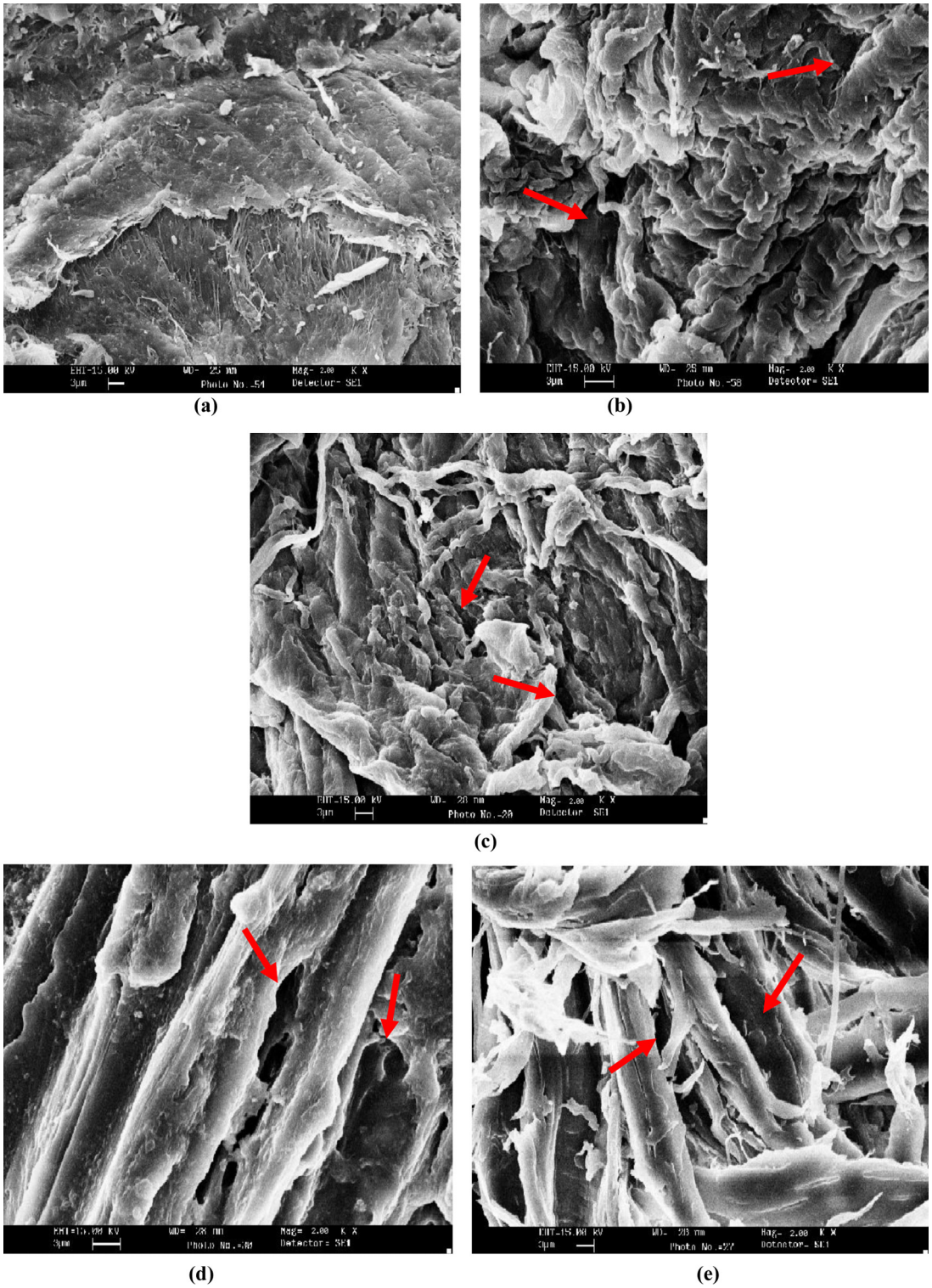

Fig. 1. Scanning electron microscopic analysis of crab shell chitin (a), superfine chitin (b), amorphous chitin (c), phosphoric acid treated (d) and colloidal chitin (e).

Table 2
X-ray diffraction analysis and crystalline index of crab shell chitin before and following chemical treatment.

Chitin samples	2θ (°)	d-Spacing (Å)	CrI_{020} (%)	CrI_{110} (%)
Crab shell chitin	9.21, 19.30, 27.31	9.58, 5.64, 3.09, 2.94	84.01	89.08
Phosphoric acid treated chitin	9.01, 11.70, 19.21, 25.91	9.58, 4.61, 4.27, 3.39	71.86	74.85
Superfine chitin	9.10, 19.11, 32.41	9.29, 4.58, 3.23	66.66	71.08
Amorphous chitin	9.11, 19.07, 31.71, 34.31	9.87, 7.68, 5.12, 3.91	64.94	69.97
Colloidal chitin	9.20, 12.11, 19.00, 26.21	9.50, 6.94, 4.57, 3.37	68.64	73.72

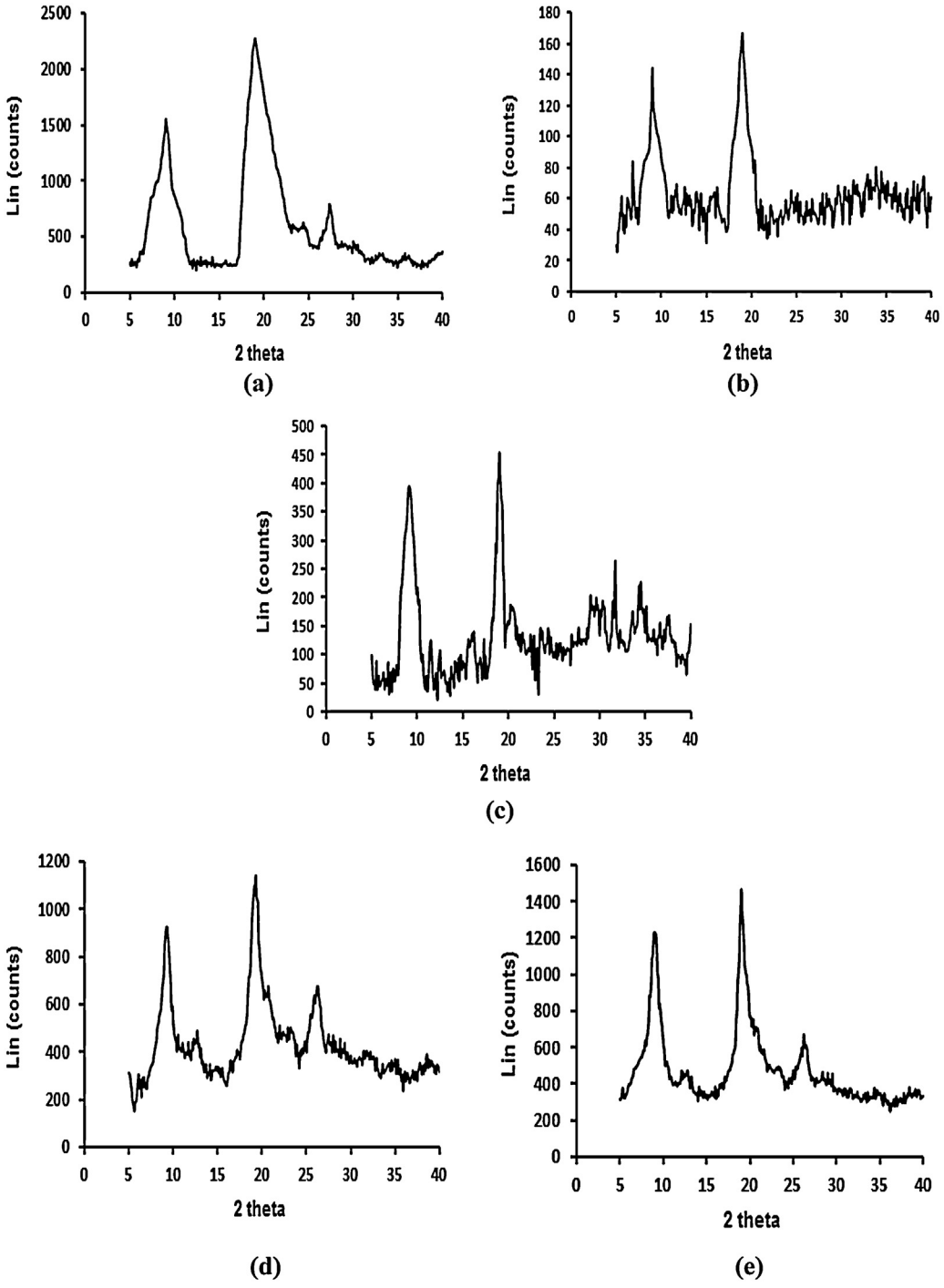

Fig. 2. X-ray diffraction analysis of crab shell chitin (a), superfine chitin (b), amorphous chitin (c), phosphoric acid treated chitin (d) and colloidal chitin (e).

the peak intensities at 9–10° and 19–20° (Table 2). Fig. 2a–e shows diffraction patterns of treated and untreated chitin. X-ray diffractograms of all the samples exhibited characteristic crystalline peaks of chitin at $2\theta \sim 9$–$10°$ and 19–20°. Some minor peaks were also observed at 27.31°, 32.41°, 34.31°, 25.91°, and 26.21° in diffractograms of the crab shell chitin, SF-CT, Am-CT, PA-CT, and Co-CT, respectively.

High crystalline index of crab shell chitin reflected its higher degree of crystallinity and more ordered structure. Both the CrI_{020} and CrI_{110} values indicated Am-CT as the most easily accessible substrate to undergo enzymatic deacetylation. Crystallinity of PA-CT and Co-CT was also observed to be significantly reduced ($\leq$70%). The order of crystallinity observed following chemical treatment was crab shell chitin > PA-CT > Co-CT > SF-CT > Am-CT. Substrate accessibility of enzyme was found to be notably improved subsequently due to the decrystallization of regular microfibrillar arrangement (Beaney et al., 2007; Martinou, Tsigos, & Bouriotis, 1997a, 1997b; Win & Stevens, 2001).

3.1.3. Thermal analysis

Chitin and chitosan are biopolymers and high thermal energy is needed for their dissociation (Bershtein & Egorov, 1994). Thermal properties of chitin samples following chemical treatment have been studied using thermogravimetric analysis (TGA) and

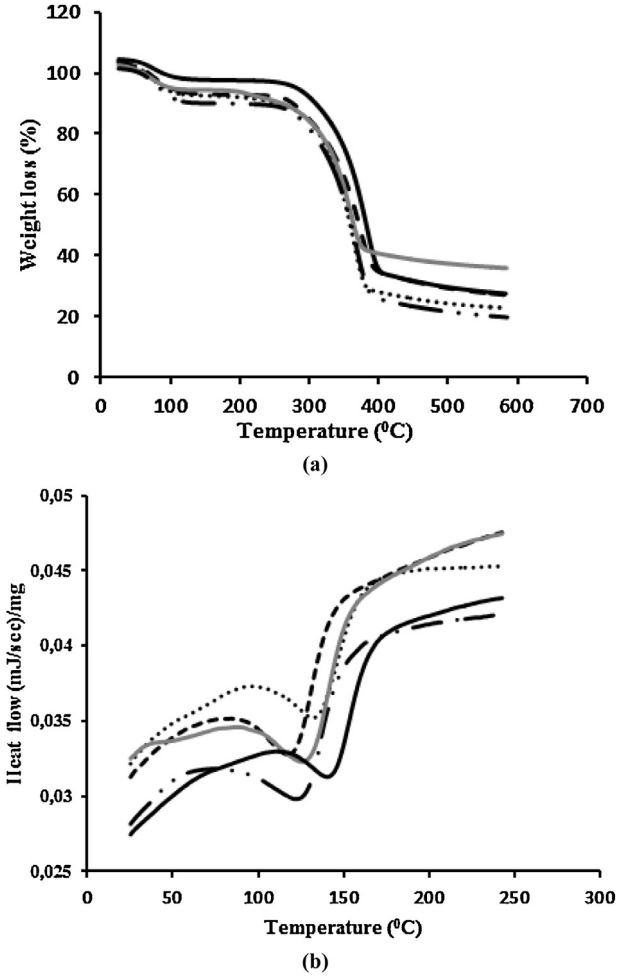

Fig. 3. TGA (a) and DSC (b) thermograms of crab shell chitin before and following chemical treatment (—, crab shell chitin; ···, phosphoric acid treated chitin; –···–, superfine chitin; - - -, amorphous chitin; ▬, colloidal chitin).

differential scanning calorimetry (DSC) (25–600 °C). TGA thermograms of all the chitinous substrates have two main decomposition stages. The first stage decomposition started at around 70 °C with weight loss of about 5.9, 6.2, 8.8, 9.4, and 8.3% for crab shell chitin, PA-CT, SF-CT, Am-CT and Co-CT, respectively (Fig. 3a). This stage is due to the loss of water content in the polysaccharide backbone. The second stage started at 270, 260, 250, 240, and 220 °C for crab shell chitin, PA-CT, Co-CT, SF-CT and Am-CT with corresponding weight loss of 66.7, 71.7, 71.9, 73.6, and 74.4%. This was due to the decomposition of the polysaccharide backbone, including acetylated and deacetylated subunits of chitin. The TGA results had indicated that crab shell chitin possesses highest thermal stability. Decrease in stability due to corresponding loss of crystallinity was observed following the chemical treatment.

DSC thermograms (30–250 °C) of chitinous substrates before and following chemical treatment had shown a wide endothermic peak around 60–240 °C with variations in the onset, peak and completion temperatures (Fig. 3b). Thermograms of chitin moieties revealed differences in endothermic peak area and positioning, indicating that the chemical treatment brings changes in the molecular structure of the polysaccharides and all the molecules exhibit varying levels of thermal stability. The variations observed also indicate differences in the water holding capacity and strength of water–polymer interaction of chitinous substrates (Guinesi & Cavalheiro, 2006; Kittur, Prashanth, Udaya Sankar, & Tharanathan, 2002; Sakurai, Maegawa, & Takahashi, 2000). Table 3 shows thermal decomposition enthalpy (ΔH) of chemically treated and untreated chitin. Amount of peak enthalpy correlated with the compactness of supra-molecular chitin structure (Jang, Kong, Jeong, Lee, & Nah, 2004; Sajomsang & Gonil, 2010). Higher enthalpy value for crab shell chitin supports its crystalline nature. Chemical treatment would result in the decrystallization of the compact structure and hence corresponding decreases in enthalpies were observed. Lowest enthalpy values of SF-CT indicated its amorphous structure and susceptibility toward thermal decomposition. Peak enthalpy values were observed to increase in the order, i.e. SF-CT < Am-CT < Co-CT < PA-CT < crab shell chitin. The discrepancy in the peak enthalpy can be attributed to the diversity of chitin fiber aggregation following chemical treatment (Jang et al., 2004). Higher peak enthalpy values revealed less susceptibility of substrate toward melting and dissociation process (Yen & Mau, 2007a, 2007b; Yen, Yang, & Mau, 2009).

3.1.4. Degree of deacetylation

DDA to a greater extent influences the performance of chitosan for a variety of applications (Aranaz et al., 2009). The FT-IR spectra of various chitinous substrates though similar to each other as a whole, however, characteristic variations were observed in the absorption intensities of the functional groups of chitin. FT-IR spectra of samples showed characteristic peaks of amide I (1655 cm^{-1}) and amide II (1560 cm^{-1}) with subtle differences in absorption intensities due to chemical treatment. The characteristic amide I peak appeared at 1658, 1656, 1654 and 1652 cm^{-1} in FT-IR spectra of PA-CT, SF-CT, Am-CT and Co-CT, respectively. Furthermore, the vibrational mode of amide II was observed at 1558, 1557, 1559 and 1568 cm^{-1}. Similar variations were also observed in the peak corresponding to 3450 cm^{-1} (—OH group). The absorption intensities corresponding to amide and hydroxyl groups were used to determine the DDA. Chitin from crab shell was observed to have about 28% of deacetylation. Extent of chitin deacetylation was significantly increased following chemical pretreatment, due to the loss of ordered crystalline structure of chitin with opening up of polymer backbone and progressive removal of acetyl groups. DDA of PA-CT and Co-CT was observed to be 32 and 33%, respectively. Am-CT generated via alkali treatment had more deformed structure hence deacetylated to marginally higher levels (34.44%). Maximum deacetylation (37.14%) was observed with SF-CT obtained following

Table 3
Differential scanning calorimetric analysis of crab shell chitin before and following chemical treatment.

Substrate	Endotherm			
	T_o (°C)	T_p (°C)	T_c (°C)	ΔH (mJ mg^{-1})
Crab shell chitin	124 ± 1.13	148 ± 1.72	188 ± 2.32	172.00 ± 0.82
Phosphoric acid treated chitin	102 ± 1.28	136 ± 1.51	179 ± 2.71	122.31 ± 0.56
Amorphous chitin	84 ± 1.41	121 ± 1.83	168 ± 1.95	95.10 ± 0.71
Superfine chitin	52 ± 1.21	116 ± 1.73	152 ± 1.60	77.20 ± 0.78
Colloidal chitin	100 ± 1.16	128 ± 1.52	161 ± 1.78	104.54 ± 0.91

T_o, onset temperature; T_p, peak temperature; T_c, completion temperature; ΔH (mJ mg^{-1}), peak enthalpy. Each value is expressed at mean ± SE (n = 3).

calcium chloride/formic acid treatment. DDA analyzed by FT-IR and elemental analysis are almost similar.

3.2. Enzymatic deacetylation

Deacetylation potential of purified *P. oxalicum* SAE_M-51 CDA on untreated crab shell chitin and chemically pretreated chitin was evaluated by incubating appropriate amount of substrate with enzyme for 24 h, samples were withdrawn at various intervals and analyzed for the amount of acetic acid released and DDA. Kinetics of enzyme reaction revealed that relatively higher extent of deacetylation was observed initially that reached to a plateau after 10 h (Fig. 4a). DDA increased marginally in the later phase even with prolonged reaction time and presence of higher amount of substrate. This might be attributed to the accessibility of acetyl groups (Stevens, Win, Ng, Pichyangkura, & Chandrkrachang, 1997). Initially the exterior acetyl groups are removed, afterwards the rate of removal decreases as the interior acetyl groups are not accessible to the enzyme and reached to a plateau. A similar deacetylation pattern was also observed with the CDA from *Colletotrichum lindemuthianum* and *Absidia coerulea* (Win & Stevens, 2001).

Untreated chitin, i.e. chitin from crab shell had the minimum level of deacetylation among all the substrates analyzed, due to its higher crystallinity, negligible porosity and closely packed structure. Similar findings were also observed during deacetylation of crab shell chitin employing CDA from *C. lindemuthianum* (Beaney et al., 2007; Martinou et al., 1995). SF-CT appeared as the most promising substrate for enzymatic deacetylation (79.52%). This might be attributed to the calcium chloride and formic acid solvent system. Lower concentrations of formic acid causes the weakening of the crystal structure of chitin and make it more amorphous to facilitate the reaction. Furthermore, the residual calcium chloride present may draw water into the structure due to its high affinity for water and it may get dissolved at reaction temperature leaving a more porous structure than its native one. Lower crystalline index and porous morphology of the substrate makes both the interior and exterior acetyl groups accessible for the enzyme. Effectiveness of the above pretreatment system to deacetylate chitin using CDA from *C. lindemuthianum* was also observed (Beaney et al., 2007).

Co-CT appeared as the second most susceptible substrate for enzymatic deacetylation (72.31%) in spite of its regular crystalline microfibrillar structure, as observed by scanning electron micrographs. Morphological examination and crystallinity of Am-CT depicted it as the second potential substrate for enzymatic action. But the deacetylation level achieved with the later was comparatively lower than that of the Co-CT. This might be due to the heterogeneous nature of the substrate, although some parts of the sample are amorphous, there would possibly be the crystalline regions within the sample causing hindrance to enzymatic action. Higher degree of crystallinity and relatively lower extent of exposed surface area affected into phosphoric acid treated chitin as the less preferred substrate for enzymatic action (62%).

3.3. Derivation of reaction conditions for enzymatic deacetylation

A significant level of deacetylation was achieved with SF-CT using purified CDA from *P. oxalicum* SAE_M-51. Further enhancement in DDA can be achieved by deriving optimal levels of critical variables viz. enzyme dose and substrate amount using 2^2 full-factorial CCD in terms of acetic acid released and DDA. Each factor in the design was studied at five levels ($-\alpha$, -1, 0, $+1$, $+\alpha$) and a set of 11 experiments was carried out. All variables were taken at a central coded value considered as zero. All experiments were conducted in triplicates and the average value was taken as the response (Y). The CCD design and the corresponding experimental data are shown in Table 1b. Results of regression analyses and ANOVA for

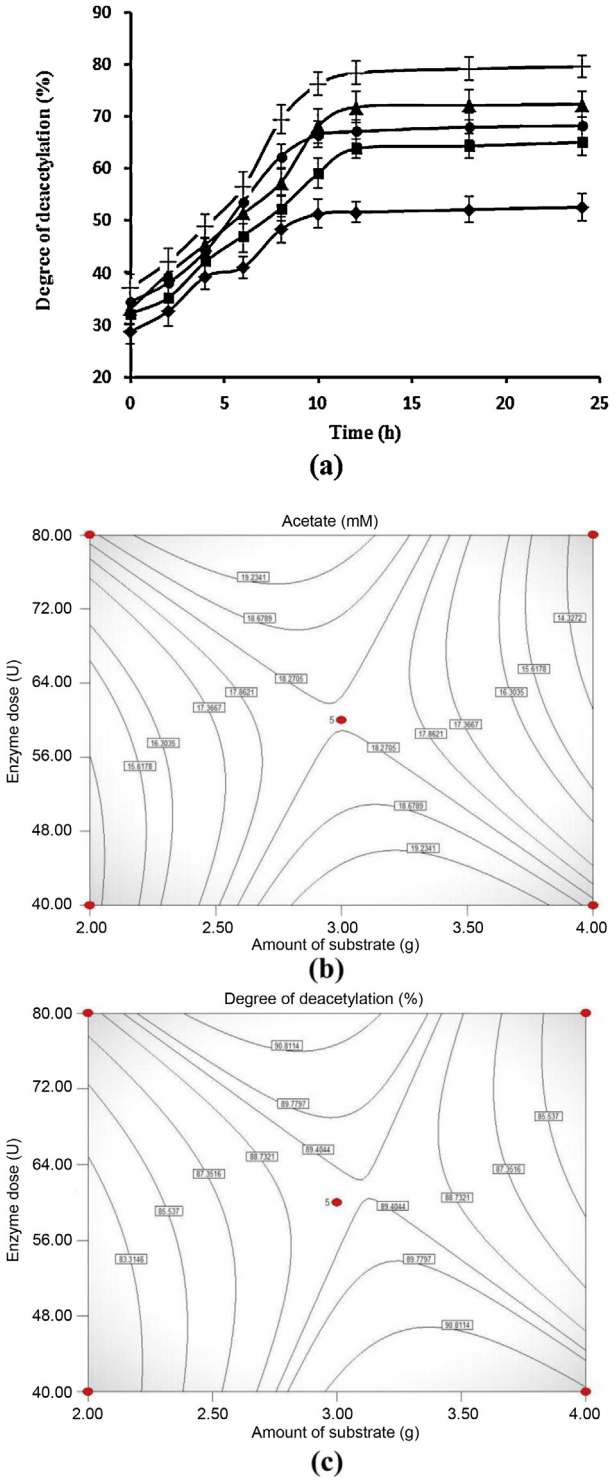

Fig. 4. Analysis of degree of deacetylation of untreated and treated chitin (a) (♦, crab shell chitin; ■, phosphoric acid treated chitin; +, superfine chitin; ●, amorphous chitin; ▲, colloidal chitin); contour plot of acetate released (b) and degree of deacetylation (c) as a function of substrate amount and enzyme dose.

acetate released (mM) and DDA (%) are presented in Tables 4a–4c. By applying multiple regression analyses on the experimental data, the following second order polynomial equations had enumerated the amount of acetic acid released (1) and DDA (2) as a function of the variables analyzed.

$$Y = 18.26 - 0.13X_1 - 0.10X_2 - 3.67X_2^1 + 1.48X_2^2 - 2.42X_1X_2 \quad (1)$$

Table 4a
Result of multiple regression analysis of central composite design.

Variables	Acetate released		DDA (%)	
	Coefficient	*P*-Value	Coefficient	*P*-Value
Intercept	18.26	–	89.31	–
X_1	−0.13	0.6585	1.52	0.0093
X_2	−0.10	0.7153	0.17	0.7101
X_1X_2	−2.42	0.0004	−3.98	0.0003
X_1^2	−3.67	<0.0001	−5.60	<0.0001
X_2^2	1.48	0.0015	1.95	0.0038

Table 4b
ANOVA for quadratic model for DDA (%).

Source	SS	DF	MS	*F*-Value	*P*-Value (prob > *F*)
Model	351.25	5	70.25	47.83	<0.0001
Residual	10.28	7	1.47	–	–
Lack of fit	10.08	3	3.36	66.85	0.0007
Pure error	0.20	4	0.050	–	–
Total	361.53	12	–	–	–

R^2: 0.9722; adj. R^2: 0.9511; C.V.: 1.39%; adeq. precision: 21.245.

Table 4c
ANOVA for quadratic model for acetate released.

Source	SS	DF	MS	*F*-value	*P*-Value (prob > *F*)
Model	144.54	5	28.91	47.85	<0.0001
Residual	4.23	7	0.60	–	–
Lack of fit	3.89	3	1.30	15.30	0.0117
Pure error	0.34	4	0.085	–	–
Total	148.77	12	–	–	–

R^2: 0.9716; adj. R^2: 0.9513; C.V.: 4.60%; adeq. precision: 20.135.

$$Y = 89.31 + 1.52X_1 + 0.17X_2 - 5.60X_2^1 + 1.95X_2^2 - 3.98X_1X_2 \quad (2)$$

The Fisher's *F*-test with a very low probability value (<0.0001) indicated that both the models were highly significant. The goodness of the fit of the model was examined by coefficient of determination (R^2) value. It was calculated to be 0.9716 for acetic acid released and 0.9722 for DDA. This implied that the sample variation of 97.16 and 97.22% was attributed to the variables and only 2.84 and 2.78% of the total variance could not be explained by the model. The adjusted R^2 values of 0.9513 for acetate released and 0.9511 for DDA were also satisfactory to denote the validity of the model. The 'adequate precision' values of and 20.13 for acetic acid released and 21.24 for DDA, respectively, indicated that the model can be used to navigate the design space. A lower value of coefficient of variation (CV = 4.60, 1.39% for acetate released and DDA, respectively) showed that the experiments conducted were reliable and precise.

The 2D contour and 3D response surface curves were plotted to understand the interaction of the variables and also to determine their optimum levels to attain maximum response. The strong interaction between amount of substrate and enzyme dose for both the responses is evident from the response surface contour plots between them (Fig. 4b and c) and also from their low corresponding probability of failure value. The predicted responses for degree of deacetylation and acetate released were 89.07% and 18.26 mM (substrate, 3.02 g; CDA, 59 U).

Validation of the model and regression equation was performed by taking the values at their optimum levels. The experimental responses (acetate released, 19.54 mM; deacetylation 90.32%) were in close agreement with the statistically predicted ones, confirming the validity of the model.

4. Conclusions

The present study emphasizes that the pretreatment of the crystalline chitin species contributes to the enzymatic biotransformation by increasing the substrate accessibility to the enzyme. Pretreatment and optimization of process variables increased the degree of deacetylation of resultant chitosan by 3.2 fold. Further, studies on mode of action and catalytic mechanism of the enzyme system along with the exploration of more effective pretreatment strategies is vital for effective bioconversion for production of chitosan with desired degree of deacetylation.

Acknowledgement

NP gratefully acknowledges the fellowship support by Council of Scientific and Industrial Research, New Delhi, India.

References

Arakane, Y., Taira, T., Ohnuma, T., & Fukamizo, T. (2012). Chitin-related enzymes in agro-biosciences. *Current Drug Targets*, *13*, 442–470.
Aranaz, I., Mengibar, M., Harris, R., Parios, I., Miralles, B., Acosta, N., et al. (2009). Functional characterization of chitin and chitosan. *Current Chemical Biology*, *3*, 203–230.
Aye, K. N., Karuppuswamy, R., Ahamed, T., & Stevens, W. F. (2006). Peripheral enzymatic deacetylation of chitin and reprecipitated chitin particles. *Bioresource Technology*, *97*, 577–582.
Beaney, P. D., Gan, Q., Magee, T. R. A., Flealy, M., & Lizardi-Mendoza, J. (2007). Modification of chitin properties for enzymatic deacetylation. *Journal of Chemical Technology and Biotechnology*, *82*, 165–173.
Bershtein, V. A., & Egorov, V. M. (1994). Differential scanning calorimetry of polymer. In *Polymer science and technology*. Chichester, UK: Ellis Horwood.
Caufrier, F., Martinou, A., Dupont, C., & Bouriotis, V. (2003). Carbohydrate esterase family 4 enzymes: Substrate specificity. *Carbohydrate Research*, *338*, 687–692.
Focher, B., Beltrame, P. L., Naggi, A., & Torri, G. (1990). Alkaline N-deacetylation of chitin enhanced by flash treatments: Reaction kinetics and structure modifications. *Carbohydrate Polymers*, *12*, 405–418.
Gou, J. X., Dong, W. B., Zeng, Q., & Zhang, J. J. (2012). Isolation and identification of strains with high chitin deacetylase activity. In S. Gao (Ed.), *Advanced materials and engineering materials, advanced materials research* (Vols. 457–458) (pp. 476–479). Stafa-Zurich: Trans Tech Publications Ltd.
Guinesi, L. S., & Cavalheiro, E. T. G. (2006). The use of DSC curves to determine the acetylation degree of chitin/chitosan samples. *Thermochimica Acta*, *444*, 128–133.
Jang, M. K., Kong, B. G., Jeong, Y. I., Lee, C. H., & Nah, J. W. (2004). Physicochemical characterization of α-chitin, β-chitin and γ-chitin separated from natural resources. *Journal of Polymer Science, Part A: Polymer Chemistry*, *42*, 3423–3432.
Kassai, M. R., Arul, J., & Charlet, G. (2000). Intrinsic viscosity–molecular weight relationship for chitosan. *Journal of Polymer Science, Part B: Polymer Physics*, *38*, 2591–2598.
Khan, T. A., Peh, K. K., & Cing, H. S. (2000). Mechanical bioadhesive strength and biological evaluation of chitosan films for wound dressing. *Journal of Pharmaceutical Sciences*, *3*, 3003–3371.
Kittur, F. S., Prashanth, K. V., Udaya Sankar, K., & Tharanathan, R. N. (2002). Characterization of chitin, chitosan and their carboxymethyl derivatives by differential scanning calorimetry. *Carbohydrate Polymers*, *49*, 185–193.
Kolodziejska, I., Wojtasz-Pajak, A., Ogonowska, G., & Sikorski, Z. E. (2000). Deacetylation of chitin in a two-stage chemical and enzymatic process. *Bulletin of the Sea Fisheries Institute*, *2*, 15–24.
Kumar, N. N., Muzzarelli, R. A. A., Muzzarelli, C., Sashiwa, H., & Domb, A. J. (2004). Chitosan chemistry and pharmaceutical perspectives. *Chemical Reviews*, *104*, 6017–6084.
Liu, J. N., & He, Y. H. (2011). Study on enzymatic characteristics of chitin deacetylase. In Z. Cao, Y. He, L. Sun, & X. Cao (Eds.), *Application of chemical engineering, advanced materials research* (Vols. 236–238) (pp. 996–999). Stafa-Zurich: Trans Tech Publications Ltd.
Mao, J. S., Cui, Y. L., Wang, X. H., Sun, Y., Yin, Y. J., Zhao, H. M., et al. (2004). A preliminary study on chitosan and gelatin polyelectrolyte complex cytocompatibility by cell cycle and apoptosis analysis. *Biomaterials*, *25*, 3973–3981.
Martinou, A., Kafetzopoulos, D., & Bouriotis, V. (1995). Chitin deacetylation by enzymatic means: Monitoring of deacetylation process. *Carbohydrate Research*, *273*, 235–242.
Martinou, A., Tsigos, I., & Bouriotis, V. (1997a). Enzymatic deacetylation of chitooligosaccharides. In R. A. A. Muzzarelli, & M. G. Peter (Eds.), *Chitin handbook* (pp. 191–194). Atec: Grottammare, Italy.
Martinou, A., Tsigos, I., & Bouriotis, V. (1997b). Preparation of chitosan by enzymatic deacetylation. In R. A. A. Muzzarelli, & M. G. Peter (Eds.), *Chitin handbook* (pp. 501–506). Atec: Grottammare, Italy.
Muzzarelli, R. A. A. (2011). Chitin nanostructures in living organisms. In S. N. Gupta (Ed.), *Chitin formation and diagenesis* (Vol. 34) (pp. 1–34). Dordrecht: Springer.

Muzzarelli, R. A. A., Boudrant, J., Meyer, D., Manno, N., DeMarchis, M., & Paoletti, M. G. (2012). Current views on fungal chitin/chitosan, human chitinases, food preservation, glucans, pectins and inulin: A tribute to Henri Braconnot, precursor of the carbohydrate polymers science, on the chitin bicentennial. *Carbohydrate Polymers*, *87*, 995–1012.

Nessa, F., Masum, S. M., Asaduzzaman, M., Roy, S. K., Hossain, M. M., & Jahan, M. S. (2010). A process for the preparation of chitin and chitosan from prawn shell waste. *Bangladesh Journal of Scientific and Industrial Research*, *45*, 323–330.

No, H. K., Cho, Y. I., Kim, H. R., & Meyers, S. P. (2000). Effective deacetylation of chitin under conditions of 15 psi/121 °C. *Journal of Agricultural and Food Chemistry*, *48*, 2625–2627.

Pareek, N., Vivekanand, V., Dwivedi, P., & Singh, R. P. (2011). *Penicillium oxalicum* SAEM-51: A mutagenised strain for enhanced production of chitin deacetylase for bioconversion to chitosan. *New Biotechnology*, *28*, 118–124.

Pareek, N., Vivekanand, V., Saroj, S., Sharma, A. K., & Singh, R. P. (2012). Purification and characterization of chitin deacetylase from *Penicillium oxalicum* SAEM-51. *Carbohydrate Polymers*, *87*, 1091–1097.

Sajomsang, W., & Gonil, P. (2010). Preparation and characterization of α-chitin from cicada sloughs. *Materials Science and Engineering C*, *30*, 357–363.

Sakurai, K., Maegawa, T., & Takahashi, T. (2000). Glass transition temperature of chitosan and miscibility of chitosan/poly(N-vinyl pirrolidone) blends. *Polymer*, *41*, 7051–7056.

Stevens, W. F., Win, N. N., Ng, C. H., Pichyangkura, C., & Chandrkrachang, S. (1997). Towards technical biocatalytic deacetylation of chitin. In A. Domard, G. A. F. Roberts, & K. M. Varum (Eds.), *Advances in chitin science* (pp. 40–47). Jacques Andre: Lyon.

Tokuyasu, K., Ohnishi-Kameyama, M., & Hayashi, K. (1996). Purification and characterization of extracellular chitin deacetylase from *Colletotrichum lindemuthianum*. *Bioscience, Biotechnology and Biochemistry*, *60*, 1598–1603.

Tsigos, I., Martinou, A., Kafetzopoulos, D., & Bouriotis, V. (2000). Chitin deacetylases: New, versatile tools in biotechnology. *Trends in Biotechnology*, *18*, 305–312.

Vaaje-Kolstad, G., Horn, S. J., van Aalten, D. M. F., Synstad, B., & Eijsink, V. G. H. (2005). The non-catalytic chitin-binding protein CBP21 from *Serratia marcescens* is essential for chitin degradation. *The Journal of Biological Chemistry*, *280*, 28492–28497.

Vaaje-Kolstad, G., Houston, D. R., Riemens, A. H. K., Eijsink, V. G. H., & Aalten, D. M. F. (2005). Crystal structure and binding properties of the *Serratia marcescens* chitin-binding protein CBP21. *The Journal of Biological Chemistry*, *280*, 11313–11319.

Vaaje-Kolstad, G., Westereng, B., Horn, S. J., Liu, Z., Zhai, H., Sorlie, M., et al. (2010). An oxidative enzyme boosting the enzymatic conversion of recalcitrant polysaccharides. *Science*, *330*, 219–222.

Win, N. N., Pengju, G., & Stevens, W. F. (2000). Deacetylation of chitin by fungal enzymes. In M. G. Peter, A. Domard, & R. A. A. Muzzarelli (Eds.), *Advances in chitin science* (pp. 55–62). Postdam: University of Postdam.

Win, N. N., & Stevens, W. F. (2001). Shrimp chitin as substrate for fungal chitin deacetylase. *Applied Microbiology and Biotechnology*, *57*, 334–341.

Yen, M. T., & Mau, J. L. (2007a). Physico-chemical characterization of fungal chitosan from shiitake stipes. *LWT-Food Science and Technology*, *40*, 472–479.

Yen, M. T., & Mau, J. L. (2007b). Selected physical properties of chitin prepared from shiitake stipes. *LWT-Food Science and Technology*, *40*, 558–563.

Yen, M. T., Yang, J. H., & Mau, J. L. (2009). Physicochemical characterization of chitin and chitosan from crab shells. *Carbohydrate Polymers*, *75*, 15–21.

Zhao, Y., Park, R. D., & Muzzarelli, R. A. A. (2010). Chitin deacetylases: Properties and applications. *Marine Drugs*, *8*, 24–46.